Role of Charges on Cytochrome *f* from the Cyanobacterium *Phormidium laminosum* in Its Interaction with Plastocyanin[†]

Sarah E. Hart,[‡] Beatrix G. Schlarb-Ridley,*[,‡] Christine Delon,[§] Derek S. Bendall,[‡] and Christopher J. Howe[‡]

Department of Biochemistry and Cambridge Centre for Molecular Recognition, University of Cambridge, Cambridge, CB2 1QW, United Kingdom, and Signalling Programme, Babraham Institute, Babraham, Cambridge, CB2 4AT, United Kingdom

Received November 22, 2002; Revised Manuscript Received March 13, 2003

ABSTRACT: The role of charge on the surface of cytochrome *f* from the cyanobacterium *Phormidium laminosum* in the reaction with plastocyanin was investigated in vitro using site-directed mutagenesis. Charge was neutralized at five acidic residues individually and introduced at a residue close to the interface between the two proteins. The effects on the kinetics of the reaction were measured using stopped-flow spectrophotometry, and the midpoint potentials of the mutant proteins were determined. The dependence of the bimolecular rate constant of reaction, k_2, on ionic strength was determined for the reactions of the cytochrome *f* mutants with wild-type and mutant forms of plastocyanin. Double mutant cycle analysis was carried out to probe for the presence of specific electrostatic interactions. The effects of mutations on Cyt *f* were smaller than those seen previously for mutants of plastocyanin [Schlarb-Ridley, B. G. et al. (2002) *Biochemistry 41,* 3279−3285]. One specific short-range interaction between charged residues of wild-type plastocyanin (Arg93) and wild-type cytochrome *f* (Asp63) was identified. The kinetic evidence from this study and that of Schlarb-Ridley et al., 2002, appears to conflict with the NMR structure of the *P. laminosum* complex, which suggests the absence of electrostatic interactions in the final complex [Crowley, P. et al. (2001) *J. Am. Chem. Soc. 123,* 10444−10453]. The most likely explanation of the apparent paradox is that the overall rate is diffusion controlled and that electrostatics specifically influence the encounter complex and not the reaction complex.

Cytochrome *f* and Plastocyanin (Pc)[1] are part of the electron-transfer chain that links the two photosystems of oxygenic photosynthesis. Cytochrome *f*, which exists as an integral component of the cytochrome *bf* complex, accepts electrons from the Rieske protein and passes them on to P_{700}^+ of photosystem I via Pc, a lumenal electron carrier.

The interaction between Pc and cytochrome *f* is weak to ensure that dissociation of the proteins does not limit turnover of the electron-transfer chain. However, the interaction must be specific enough to allow a close approach of the redox centers; electron transfer is highly distance dependent (*1*). Our study focuses on the role of charge in the interaction between cytochrome *f* and Pc of *Phormidium laminosum*, a moderately thermophilic cyanobacterium.

The redox-active, N-terminal domain of cytochrome *f* (referred to here as Cyt *f*) protrudes into the thylakoid lumen and is anchored to the thylakoid membrane by a single transmembrane helix. Expressed independently, this domain of 28 kDa is soluble and has been used in the present study. Its crystal structure shows it to consist of antiparallel β-sheets that form two subdomains (*2*). The amide of Tyr1 directly ligates the heme iron, which has been found in all cytochromes *f* crystallized so far (*3*, *4*). Although the protein is structurally well-conserved among plants, algae, and cyanobacteria, the surface charge properties of Cyt *f* are not (*2*). The soluble fragment of the turnip protein has a net charge of −1 at pH 7 (*5*), whereas the equivalent *P. laminosum* fragment has a net charge of −12 at the same pH (*6*). A conserved basic ridge is present in higher plant and algal Cyt *f* (*3*) but is replaced with more diffusely arranged acidic residues in *P. laminosum* Cyt *f*.

Pc is a lumenal protein of about 11 kDa, with a highly conserved antiparallel β-barrel structure (*7*, *8*). The copper center is buried 6 Å below a hydrophobic surface region. Like Cyt *f*, the surface charge properties of Pc are not conserved, whereas the overall structure is. Higher plant Pcs have a net charge of -9 ± 1 at pH 7 (*9*), whereas cyanobacterial Pcs have widely varying net charges. *P. laminosum* Pc has a net charge of −1 at pH 7 (*10*). One face of higher plant Pc is occupied by two acidic patches. The analogous region of *P. laminosum* Pc is occupied by both acidic and basic residues. Previous studies have shown that these differences in surface charge properties have a profound influence on the kinetics of the interaction (*11*).

[†] This work was supported by the Biotechnology and Biological Sciences Research Council, the Deutscher Akademischer Auslandsdienst (Doktorandenstipendium im Rahmen des gemeinsamen Hochschulsonderprogramms III von Bund und Ländern), the Oppenheimer Trust, and Corpus Christi College, Cambridge.

* Corresponding author. Tel.: ++44 1223 333687. Fax: ++44 1223 333345. E-mail: bgs9@mole.bio.cam.ac.uk.

[‡] University of Cambridge.

[§] Babraham Institute.

[1] Abbreviations: Cyt *f*, soluble redox-active domain of cytochrome *f*; E_m, midpoint potential; *P. laminosum*, *Phormidium laminosum*; Pc, plastocyanin; wt, wild type.

10.1021/bi020674h CCC: $25.00
Published on Web 04/05/2003

The structure of the transient complex formed between spinach Pc and turnip Cyt *f* in vitro has been determined, using paramagnetic NMR and restrained rigid body molecular dynamics (*12*). van der Waals contact between the heme region of Cyt *f* and the hydrophobic patch of Pc brings the two metal ions, Fe and Cu, within about 11 Å of each other. Interaction is also seen between the basic ridge of Cyt *f* and the acidic patches of Pc. Site-directed mutagenesis of residues within either of these two regions (*13*−*16*), which neutralizes or reverses charge at specific residues, results in a decrease in the rate of electron transfer in vitro.

Recently, the structure of the *P. laminosum* complex was determined by a similar method (*17*). The complex is less well-defined than its higher plant counterpart, either because it is more dynamic or because insufficient restraints were available. The structure and binding affinity are independent of ionic strength, suggesting a negligible contribution by electrostatic interactions, in contrast to the complex of the higher plant proteins. Contact is seen only between the hydrophobic patch of Pc and the heme region of Cyt *f*. None of the 25 lowest energy structures is homologous to the angiosperm complex.

However, kinetic measurements indicate the existence of a weak electrostatic attraction between Pc and Cyt *f* of *P. laminosum* (*11, 18*). Therefore, any kinetic model for the overall electron transfer must be able to reconcile this with the presence of exclusively hydrophobic interactions in the final complex. The current kinetic model for the interaction is given in Scheme 1. In the present work, a series of charge alteration mutants of Cyt *f* and Pc from *P. laminosum* have been analyzed, with charge neutralized at regions corresponding to the higher plant basic ridge and acidic patches, respectively. These regions were identified as being likely candidates for involvement in an electrostatic interaction, based on the interactions of the higher plant proteins.

Scheme 1

$$Pc_{ox} + Cyt\,f_{red} \underset{k_{off}}{\overset{k_{on}}{\rightleftharpoons}} [Pc_{ox}\ Cyt\,f_{red}] \underset{k_{-et}}{\overset{k_{et}}{\rightleftharpoons}} [Pc_{red}\ Cyt\,f_{ox}] \longrightarrow Pc_{red} + Cyt\,f_{ox}$$

In a previous study, neutralization and reversal of charge at the surface of Pc in the region analogous to the acidic patches was seen to affect the kinetics of the interaction (*11*). Arg93, in particular, was found to be a key determinant of rate.

In the present work, these observations have been complemented by a study of the role of charge on Cyt *f* in the interaction using stopped-flow spectrophotometry. In addition, the presence or absence of additivity between Pc and Cyt *f* mutations, as identified through double mutant cycle analysis (*16*), has been used to clarify the role of specific short-range interactions between charged residues of Pc and charged residues of Cyt *f*.

MATERIALS AND METHODS

Molecular Biology and Mutagenesis. Molecular biological methods were essentially as described by Ausubel et al. (*19*). The plasmid encoding the wild-type (wt) Cyt *f*, pUCfWT, was formerly referred to as pUC19li5 (*6*, *20*). Mutagenesis of the *petA* gene in the pUCfWT vector was carried out according to the Stratagene QuikChange mutagenesis method (*21*). The following codon changes were introduced to obtain the respective mutations: CAA to CGT for Q7R, CAA to GAA for Q7E, GAT to GCT for D63A, GAA to GCC for E165A, GAC to GCC for D187A, GAC to GCC for D188A, and GAA to GCC for E192A. Incorporation of the correct mutations and absence of undesired mutations was checked by sequencing of the mutated constructs. The plasmids with the correct mutations were named pUCfQ7R, pUCfQ7E, pUCfD63A, pUCfE165A, pUCfD187A, pUCfD188A, and pUCfE192A and were transformed into *Escherichia coli* strain DH5α.

Protein Methods. Expression, purification, and characterization of wt and mutant Cyt *f* were carried out essentially as in Schlarb et al. (*6*) or Crowley et al. (*17*). Modifications to the latter include the use of *E. coli* W3110 cells for expression and addition of chloramphenicol to a final concentration of 22 mg/L to the expression medium. W3110 cells were transformed with the Cyt *f* constructs and also the pEC86 plasmid (*22*), which increases expression of Cyt *f* in *E. coli* cells (*17*). Purification was carried out by ion-exchange chromatography (Pharmacia HiTrap Q FPLC-column of 5 × 5 mL columns in series, gradient 0−200 mM NaCl, 50 mM Tris, pH 7.5, 23 ± 1 °C) followed by gel-filtration chromatography (Pharmacia HiLoad 16/60, Superdex 75 prep grade, 100 mM NaCl, 50 mM Tris, pH 7.5 at 4 °C). Estimates of concentration were derived from the absorption at 555.6 nm for reduced Cyt *f* ($\epsilon = 31\,500\ M^{-1}\ cm^{-1}$) and 598 nm for oxidized Pc ($\epsilon = 4700\ M^{-1}\ cm^{-1}$). The purity of the isolated Cyt *f* was assessed by determining the ratio of $A_{280}/A_{555.6}$; proteins that had a ratio below 1.1 were used for the kinetic analysis. The purity of the isolated Pc was estimated from the ratio of A_{280}/A_{598}; proteins with a ratio below 2.6 were used for the kinetic analysis.

Kinetic Analysis. Measurements of the second-order rate constant, k_2, and its ionic strength dependence were performed at 300 K and pH 6.0 in an Applied Photophysics stopped-flow spectrophotometer (SF.17MV). Conditions and experimental procedures were essentially as in Schlarb-Ridley et al. (*11*). The concentration of Cyt *f* in the reaction mixture was kept at 0.1 μM. The concentrations of Pc in the reaction mixture for the ionic strength dependence were at least 10 times in excess of the Cyt *f* concentration and are stated in the legend to Figure 4. To visualize the trend, the data were fitted to the monopole−monopole version of the Watkins equation (*23*).

Redox Potentiometry. The determination of the midpoint potentials of the *P. laminosum* Cyt *f* was carried out as described in ref *11*. The midpoint redox potentials were determined at 300 ± 1 K, pH 6.0 in 90 mM KCl, 10 mM KPi, pH 6.0. The potential was adjusted with 0.1−1 μL aliquots of 10 mM ascorbate. In this current work, we have achieved greater oxygen exclusion by the use of copper tubing and increased sealing of the reaction vessel, and we attribute the more positive potential of wt *P. laminosum* Cyt *f* as compared to that reported by Schlarb-Ridley et al. (*11*) to this.

Electrostatic Potentials. Electrostatic potentials of wt and mutant forms of reduced cytochromes *f* and oxidized Pc were calculated by a finite difference solution of the linear Poisson−Boltzmann equation with DelPhi II (*24*). The Swiss-PDBViewer was used to add polar and aromatic ring hydrogens to PDB file 1ci3 (Cyt *f*) and to chain A of PDB

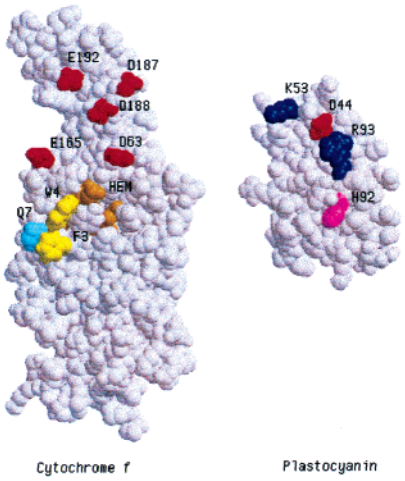

FIGURE 1: Space-filling representation of Cyt *f* and Pc of *P. laminosum*, showing acidic residues that were mutated to Ala in red. Color code for other highlighted features: yellow, Phe3 and Trp4; orange, heme; cyan, Gln7; dark blue, Lys53 and Arg93; and magenta, His92. van der Waals surfaces have been rendered by Molscript (*36*) and Raster3D (*37*).

file 1baw (Pc) and was also used to introduce mutations. Atomic radii and partial charges were assigned from the PARSE list of Sitkoff et al. (*25*), and the protein dielectric constant was set to 4.

RESULTS

Five acidic residues on *P. laminosum* Cyt *f* were selected from a region which is to one side of the heme and which would contain the basic ridge in the higher plant protein: Asp63, Glu165, Asp187, Asp188, and Glu192 (see Figure 1). To investigate the influence of these residues on the overall rate of reaction, their charge was neutralized by replacement with the small hydrophobic amino acid alanine. Alanine substitution is discussed in Wells (*26*). In addition, the conserved residue Gln7 was mutated to both Glu and Arg, to examine the effect of introducing charge close to the interface. In the 3-D structure of Cyt *f*, Gln7 sits adjacent to Phe3 and Trp4. Phe3 and Trp4 influence the kinetics of the interaction between Pc and Cyt *f* (*39*), and Trp4 influences the position of the α-band and the midpoint potential of the reduced spectrum of cytochrome *f* (*20*). Molecular masses of purified proteins as determined by ESI-mass spectroscopy (data not shown) were in agreement with the values predicted from the translated DNA sequences. The results of the isoelectric focusing (data not shown) were as expected, in that the Q7R, D63A, D187A, D188A, and E192A Cyt *f* all ran at a higher p*I* than wt Cyt *f*, and Q7E Cyt *f* ran at a slightly lower p*I*. The visible spectra of the mutants were essentially identical to those of the wt (data not shown). These results indicate that the mutant proteins were expressed correctly and that the electronic structure of the redox center was maintained. The midpoint potentials of each of the proteins are shown in Table 1. None of them differed significantly from that of wt.

Second-Order Rate Constants and Their Dependence on Ionic Strength. In all cases, the observed pseudo-first-order rate constants for the reactions between wt or mutant Cyt *f* with wt Pc showed linear responses to increasing Pc concentration (Figure 2). Values for the second-order rate constant, k_2, calculated from the slopes of these lines are

Table 1: Second-Order Rate Constants for the Reaction of wt and Mutant *P. laminosum* Cyt *f* with wt *P. laminosum* Pc[a] and Midpoint Potentials (E_m in mV) for wt and Mutant *P. laminosum* Cyt *f*[b]

Cyt *f*	k_2 (10^7 $M^{-1}s^{-1}$)	E_m (mV) ± 5
wt	4.0	331
Q7R	2.9	333
Q7E	4.0	327
D63A	3.1	338
E165A	3.9	330
D187A	3.8	329
D188A	4.2	333
E192A	4.1	330

[a] All measurements were done at 300 ± 1 K in the appropriate buffer at pH 6.0, as described in the text. The overall error of k_2 is estimated to be ≤5% of the given values; this estimate is based on the standard error of the wt measurements (*11*). [b] All measurements were done at pH 6.0 and 300 ± 1 K as described in the text. The standard error of the wt midpoint potential was determined from 3-fold repetition of the titration and applied to the mutants.

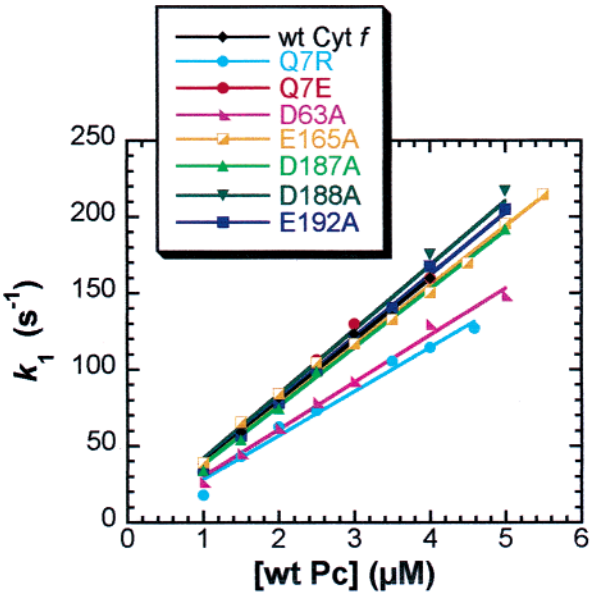

FIGURE 2: Concentration dependence of k_1: wt and mutant *P. laminosum* Cyt *f* with wt *P. laminosum* Pc. The values of k_2 were obtained from the data by linear regression through the origin and are given in Table 1. Experimental conditions: 300 ± 1 K in 10 mM KPi, 90 mM NaCl at pH 6.0; concentration of Cyt *f*, 0.1 μM.

recorded in Table 1. The mutant cytochromes *f* showed only small deviations from wt. With the exception of Q7E, which gave the same rate as wt Cyt *f*, all the mutants tested involved the loss of one negative charge (D63A, E165A, D187A, D188A, E192A) or the gain of one positive charge (Q7R). Although the differences were small at most, Figure 2 shows two distinct groups of mutants. Rates obtained for E165A, D187A, D188A, and E192A were not significantly different from that of wt, whereas Q7R and D63A were clearly slower. The last two residues were those closest to the heme Fe. In view of the difference obtained with Q7R, the effect of Q7E, which gave a rate very similar to wt, seemed anomalous, but the expected stimulation of rate became apparent at lower values of ionic strength (see below). The results therefore suggested a limited differential importance of charged residues, depending on their position on the surface of Cyt *f*.

The effect of ionic strength on k_2 for the reaction of wt or mutant Cyt *f* with wt Pc is shown in Figure 3. In all cases,

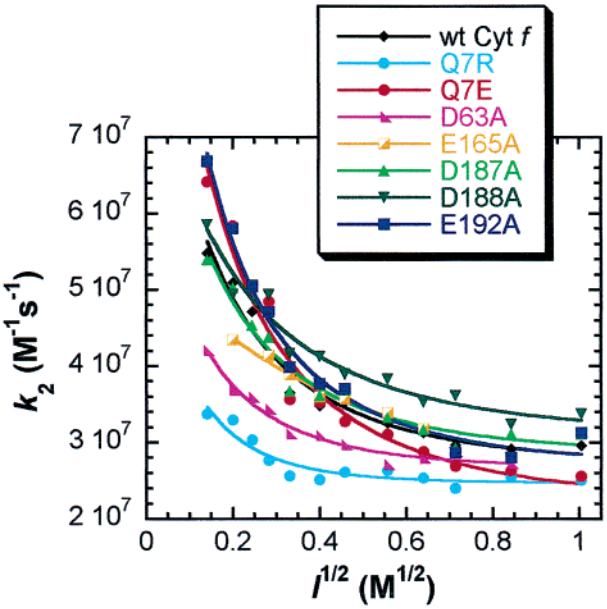

FIGURE 3: Ionic strength dependence of k_2: wt and mutant *P. laminosum* Cyt *f* reacting with wt *P. laminosum* Pc. Measurements were made at 300 ± 1 K in 20 mM MES buffer at pH 6.0. Concentration of Cyt *f*, 0.1 μM; concentration of wt Pc, ≥10× the concentration of Cyt *f*. The concentration of NaCl was varied from 0 to 1.0 M. The data were fitted to the Watkins equation, excluding the first data point (not shown). This exclusion is discussed in Schlarb-Ridley et al. (*11*).

k_2 decreased with increasing ionic strength, which indicated an electrostatic attraction between the reactants. The curves obtained with the mutants fell into two main groups, with E165A, D187A, D188A, and E192A clustering around the wt curve, whereas Q7R and D63A fell into a discrete group showing a less marked electrostatic attraction. Thus, again, it may be concluded that charges at positions 7 or 63 have a noticeable effect, but when further away from the heme any effect is small. The behavior of Q7E was distinct from that of the other mutants. At lower ionic strength it gave the expected stimulation compared with wt, but the wt and Q7E curves crossed at $I = 0.16$ M, so that the mutant gave slower rates at higher ionic strength. The curve for Q7E thus appeared to be displaced downward on the k_2 axis. The interpretation of this displacement, which can also be seen in the curve for Q7R, is not clear.

Specific Charge−Charge Interactions between Cyt f and Pc. Ionic strength effects were exploited further to examine the possibility of specific interactions between charged side chains of Cyt *f* and of Pc. Asp44, Asp45, Lys46, Lys53, and Arg93 of Pc have already been shown to interact with wt Cyt *f* by the effects of single mutations, the strongest effects being observed with mutants of Arg93. The ionic strength dependence was therefore determined for selected Pc mutants reacting with mutants of Cyt *f* to establish whether the effects of the two single mutations were additive in the double mutant reaction (mutant Cyt *f*/mutant Pc). Nonadditivity would be indicative of a specific interaction between the two charged side chains. This double mutant analysis is based on the principle that the change in charge mutation of two interacting residues, one from each protein, is not expected to have an additive effect on rate. It reflects the fact that the specific interaction between the two residues is eliminated with the mutation of just one of the residues.

Scheme 2[a]

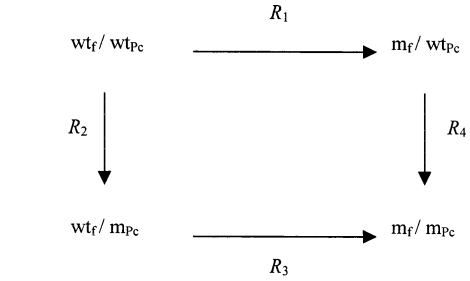

$$R_1 = \frac{k_2\,(m_f/\,wt_{Pc})}{k_2\,(wt_f/\,wt_{Pc})} \qquad R_2 = \frac{k_2\,(wt_f/\,m_{Pc})}{k_2\,(wt_f/\,wt_{Pc})}$$

$$R_3 = \frac{k_2\,(m_f/\,m_{Pc})}{k_2\,(wt_f/\,m_{Pc})} \qquad R_4 = \frac{k_2\,(m_f/\,m_{Pc})}{k_2\,(m_f/\,wt_{Pc})}$$

$$R_{int} = R_3/R_1 = R_4/R_2$$

[a] Adapted from Gong et al. (*16*), where wt_f = wild-type Cyt *f*, m_f = mutant Cyt *f*, wt_{Pc} = wild-type Pc, and m_{Pc} = mutant Pc.

Therefore, mutation of the second residue will not affect the specific interaction. The effect seen with the double mutation will always be less than the sum of the effects seen with the single mutations. In contrast, mutation of two noninteracting residues should produce an additive effect. We have applied the double mutant analysis to the ionic strength curves because these give a measure of the electrostatic interactions. Results obtained with mutant pairs showing the most clear-cut effects are shown in Figure 4. Figure 4a shows that Asp187 of Cyt *f* does not interact with Arg93 of Pc because the D187A mutation had little or no effect whether the reaction was with wt Pc or the R93Q mutant. Similarly, R93E Pc reacted at the same rate with either wt or D187A Cyt *f* over a wide range of ionic strength. Nevertheless, loss or reversal of the charge of Arg93 had a strong effect on the reactivity with Cyt *f*, as previously shown.

On the other hand, clear evidence of nonadditivity was found between Asp63 of Cyt *f* or the Q7R or Q7E mutants and Arg93 of Pc (Figure 4b−d). Thus, the D63A mutation in Cyt *f* significantly slowed the reaction with wt Pc over the whole range of ionic strength but had no effect on the reaction with R93Q Pc. Similarly, the Q7R and Q7E mutations of Cyt *f* had larger effects in the reaction with wt Pc than with R93Q Pc. These effects were confirmed when the charge on Arg93 was inverted (R93E) rather than neutralized (R93Q). Thus, there was evidence for a specific repulsion between R93E of Pc and Asp63 of Cyt *f* and a specific attraction between R93E and Q7R. To obtain a more quantitative assay of specific interactions, the method of double mutant cycles was applied to values of k_2 measured under standard conditions (10 mM KPi, 90 mM NaCl, pH 6.0). The type of cycle employed is illustrated in Scheme 2.

R_n represents the ratio of the appropriate pair of values for k_2. An interaction ratio, R_{int}, may be defined as $R_{int} = R_3/R_1 = R_4/R_2$. For independent or additive effects $R_3 = R_1$,

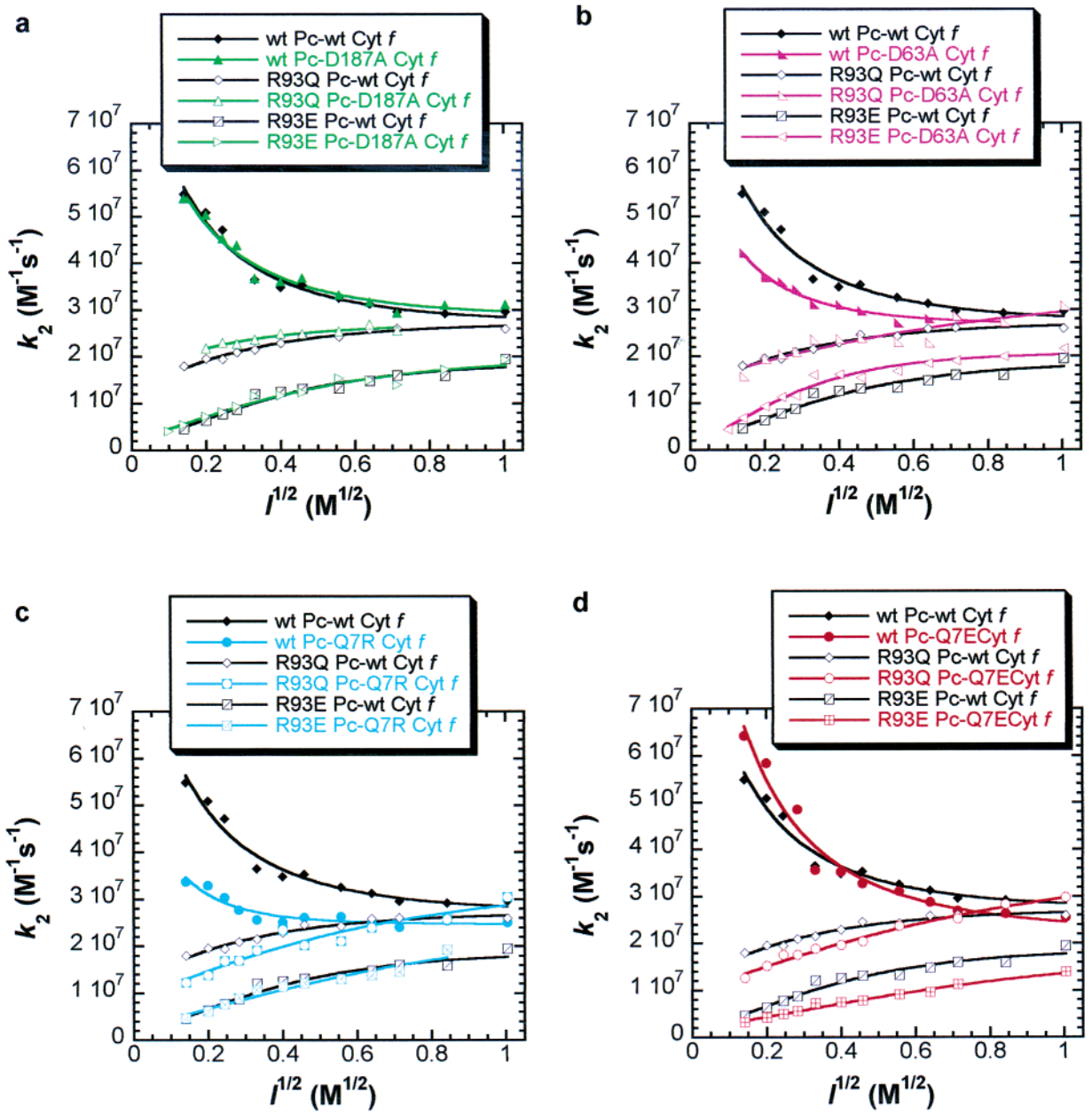

FIGURE 4: Ionic strength dependence of k_2: wt and mutant Pc reacting with wt and mutant Cyt *f*: wt, R93Q, and R93E Pc with wt and D187A Cyt *f* (a); wt, R93Q, and R93E Pc with wt and D63A Cyt *f* (b); wt, R93Q, and R93E Pc with wt and Q7R Cyt *f* (c); wt, R93Q, and R93E Pc with wt and Q7E Cyt *f* (d). Experimental conditions: 300 ± 1 K in 20 mM MES buffer at pH 6.0; concentration of Cyt *f* and Pc were, in general, 0.1 and 1.6 μM, respectively; for the reaction of wt Cyt *f* and wt Pc the concentration of wt Pc was 1 μM, and for the reactions of wt Pc with D63A Cyt *f* and Q7E Cyt *f* the concentration of wt Pc was 1.4 μM.

$R_4 = R_2$, and $R_{int} = 1$. R_{int} is a quotient of a quotient calculated from k_2 values (as defined in Scheme 2). The error of a quotient of two measured values can be approximated by the sum of the errors of the two measured quantities (*27*). A 5% error (fractional uncertainty of 0.05) was assumed for k_2 estimates, based on previous results (*11*). Therefore, the fractional uncertainties of R_1, R_2, R_3, and R_4 are 0.1 (10%), and the fractional uncertainty of R_{int} is 0.2 (20% error). We define a significant nonadditive effect as an R_{int} value for which the probable range (R_{int} value calculated ± 0.2) does not include 1. This method of analysis confirmed the specific interaction between Asp63 of Cyt *f* and Arg93 of Pc, which had been suggested by the ionic strength effects on k_2. The mutants D63A and R93E gave $R_{int} = 2.1 \pm 0.42$. This value is clearly above the R_{int} of 1 expected for an additive effect. On the other hand, despite the evidence of nonadditivity shown in Figure 4d, the mutants Q7E and R93E gave $R_{int} = 0.7 \pm 0.14$, which is marginally significant. If viewed as a specific charge−charge interaction between Arg93 of Pc and Glu7 of the Cyt *f* mutant (i.e., Arg93 and Glu7 are taken as the reference residues), it would be equivalent to $R_{int} = 1.4$. The absence of a more clearly significant R_{int} value is due to the fact that the ionic strength used for the k_2 measurements from which R_{int} is calculated is close to the value where the wt Pc-wt Cyt *f* and wt Pc-Q7E Cyt *f* ionic strength curves intersect.

The overall conclusion from the results described in this section is that there is a specific interaction between Arg93 of plastocyanin and Asp63 of Cyt *f*, and that in the same way Arg93 is sensitive to the introduction of charge at position 7 of Cyt *f* (Q7R, Q7E). Furthermore, negatively charged residues on the surface of Cyt *f* that are further from

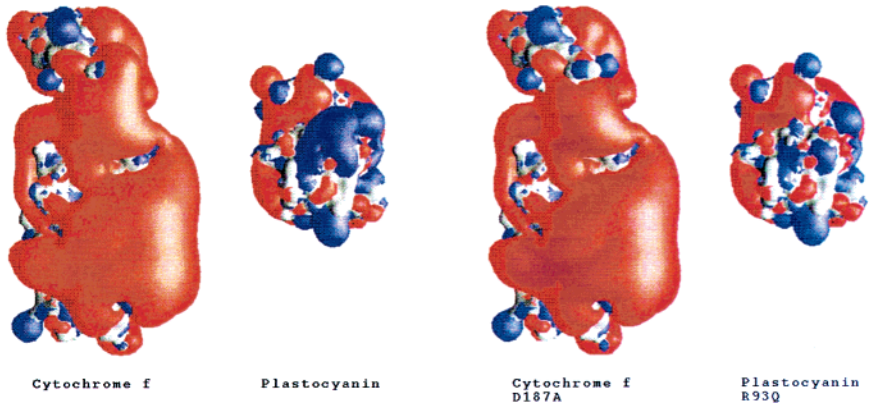

FIGURE 5: Contour plots of the electrostatic surface potentials of wt and mutant *P. laminosum* Cyt *f* and Pc at ± 1 k_BT drawn with GRASP (*38*). Red, -1 k_BT; blue, $+1$ k_BT.

the heme are relatively unimportant for the interaction between the two proteins.

DISCUSSION

In the work described above we set out to investigate the role of electrostatics in the interaction between Cyt *f* and Pc from *P. laminosum*. Kinetic studies had already demonstrated that electrostatics are much less important in the cyanobacterial case than for the homologous proteins from higher plants (*11*). The same is true for the structures of the complexes between Cyt *f* and Pc in solution, as defined by NMR experiments. Moreover, there seemed to be a contradiction between the weak but significant effects of salt on the kinetics of the reaction between the *P. laminosum* proteins and the lack of any effect on the binding constant determined by NMR, at least up to 200 mM (*18*) and within the limits of experimental error (*17*). We therefore aimed to explain the difference between the kinetics of the plant and cyanobacterial systems and to define more clearly the relatively subtle role of electrostatics in the cyanobacterial case. It was already known from mutant studies that charged groups in the region of *P. laminosum* Pc corresponding to the acidic patches of plant Pc made small contributions but that loss of the positive charge from Arg93 (corresponding to Gln88 in the plant protein) caused a more than 50% drop in rate (*11*). We expected to find that comparable effects would be observed with mutants of Cyt *f* and that an acidic residue could be identified that would interact directly with Arg93, just as an interaction between Lys187 (Cyt *f*) and Asp51 (Pc) has been identified for the plant proteins by double mutant cycle analysis (*16*).

Taking the measurements on k_2 as a whole, for the series of mutants of Cyt *f* reacting with wt Pc, the most striking result was that the effects were small as compared with those obtained with a comparable series of charge mutants of Pc reacting with wt Cyt *f*. A contour plot of the electrostatic potential surrounding each protein offers a possible explanation for this difference (Figure 5). The surface of Cyt *f* is predominantly negatively charged, whereas both positively and negatively charged groups occur close together on Pc. Cyt *f* shows a large and continuous negative contour surface in which loss of a single charged residue may have less effect.

Nevertheless, clear evidence for a preferred region of the large negative surface of Cyt *f* is provided by the specific interaction between Arg93 (Pc) and Asp63 (Cyt *f*). This suggests that Asp63 is closer to the electron-transfer site than the other acidic residues tested. Similarly, introduction of charge at position 7 of Cyt *f* (Q7R or Q7E) also led to specific interaction with Arg93. The magnitude of the effects was similar to that obtained from measurements of k_{on} in formation of the complex between barnase and barstar (*28*) and also from measurements of k_2 in the reaction between turnip cytochrome *f* and spinach plastocyanin (*16*), which was interpreted as being diffusion controlled, in which case k_2 is a measure of k_{on}. Larger effects might have been expected for charge−charge interactions influencing K_A. Our results thus suggest that the reaction between Cyt *f* and Pc in *P. laminosum* is also diffusion controlled (see below).

There are two possible explanations for the paradox of k_2, but not the binding constant (which influences the NMR result), being influenced by electrostatics. One type of explanation supposes that there is a significant electrostatic effect on k_{et}, for example, by favoring slightly different configurations that would influence the electronic coupling. For such an effect to be apparent in k_2 it is necessary to assume activation control, when $k_2 = K_A k_{et}$. We have argued above, however, on the basis of specific charge−charge interactions, that the reaction is diffusion controlled. This is supported by the fact that the reaction is very fast, and above an ionic strength of 200 mM faster than that of the plant proteins (which is thought to be diffusion controlled). Strong evidence for diffusion control comes from the observation that increasing relative viscosity causes an approximately proportionate decrease in k_2 (unpublished results). We therefore prefer the second type of explanation of the paradox, which depends on the reaction being diffusion controlled.

In the case of diffusion control an effect on k_2 but not on K_A can be explained if the electrostatic forces predominantly influence the encounter complex. It is now widely accepted that the formation of a specific complex between two proteins in solution passes through a looser precursor state, the encounter complex, which may be regarded as the endpoint of their diffusional interaction (*29*−*33*). The encounter complex is only partially desolvated and allows considerable relative motion of the proteins so that the more specific, final complex can be found. The encounter complex is influenced by long-range electrostatic forces between the two proteins, but the short-range forces mainly come into play only with

Scheme 3

$$Pc_{ox} + Cyt\,f_{red} \underset{k_{-a}}{\overset{k_a}{\rightleftharpoons}} [Pc_{ox} : Cyt\,f_{red}] \underset{k_{-r}}{\overset{k_r}{\rightleftharpoons}} [Pc_{ox}Cyt\,f_{red}] \underset{k_{-et}}{\overset{k_{et}}{\rightleftharpoons}} [Pc_{red}Cyt\,f_{ox}]$$

the formation of the final complex. Following Selzer and Schreiber (*34*) in their description of protein−protein association, the reaction between Cyt *f* and Pc may be described as a two-step association, followed by electron transfer (Scheme 3) where [Pc_{ox}:Cytf_{red}] represents the loose encounter complex and [Pc_{ox}Cytf_{red}] the specific reaction complex in which electron transfer occurs. The inclusion of the encounter complex is an expansion of Scheme 1 given in the introduction. The use of chemical shift changes to characterize complex formation by NMR (*17*) detects only the reaction complex because of the dynamic nature of the encounter complex. The rate constants, k_{on} and k_{off}, for the overall formation and dissociation of the reaction complex are related to the kinetics of the encounter complex by the following equations:

$$k_{on} = \frac{k_a k_r}{k_{-a} + k_r};\ k_{off} = \frac{k_{-a} k_{-r}}{k_{-a} + k_r}$$

and the binding constant, K_A, is given by

$$K_A = \frac{k_{on}}{k_{off}} = \frac{k_a k_r}{k_{-a} k_{-r}} = K_a K_r$$

where K_a and K_r represent the equilibrium constants for the two steps.

Under diffusion controlled conditions $k_r \gg k_{-a}$, and $k_f \gg k_{-a}k_{-r}/k_r$, and hence $k_2 = k_{on} = k_a$, see ref *35* and also Scheme 1 for the relation between k_f and k_{et}. The relation $k_2 = k_a$ implies that an electrostatic attraction influencing the formation of the encounter complex will be evident in k_2. On the other hand, if the final reaction complex is largely independent of electrostatics, as favored by the experimental evidence (*17*), the binding constant, K_A, is likely to be insensitive to an electrostatic attraction confined to the encounter complex. This is because an electrostatic attraction will increase k_a and decrease k_{-a} but have opposite effects on k_r and k_{-r}. We can therefore conclude that in the interaction between Cyt *f* and Pc from *P. laminosum*, electrostatics specifically influence the encounter complex and not the reaction complex.

The above analysis enables us to suggest a physical picture of the encounter process between Cyt *f* and Pc of *P. laminosum* in solution (see Figure 5). There is a weak electrostatic attraction between the positive charge on Pc centered mainly on Arg93 (see Figure 1) and the predominantly negatively charged surface of Cyt *f*. The electrostatic potential contour plots suggest free movement of Pc by two-dimensional diffusion within the large $-1\ k_BT$ contour of Cyt *f*. The outer boundary of the steering region may be represented by $\pm 1\ k_BT$ (*34*). Glu165, Asp187, Asp188, and Glu192, which lie underneath the $-1\ k_BT$ surface of the upper part of Cyt *f*, were shown individually to have little effect on k_2. This picture predicts that mutation of surface acidic residues on the lower part of Cyt *f* would similarly have little effect. The encounter complex, defined as the end point of this diffusional process, is more localized in the central region near the heme, however, as judged by the specific interactions with Asp63 and Gln7. These interactions will encourage short-range hydrophobic and van der Waals effects to come into play and pull the complex over into the configuration shown by the model of Crowley et al. (*17*).

So far as we are aware, the conclusion that electrostatics influence only the encounter complex applies uniquely to the reaction between *P. laminosum* Cyt *f* and Pc in solution at present, but we expect other examples to be found. In the case of the homologous proteins from higher plants the interaction can similarly be described as a two-step process but one in which there are two important differences from *P. laminosum*. First, the long-range electrostatic attraction influencing the formation of the encounter complex is much stronger, and second, there is a significant electrostatic influence on the final reaction complex, as shown by the NMR structure (*12*), so one would expect that electrostatic effects on K_a and K_r do not cancel out. In addition, the positively charged surface that plastocyanin has to explore on cytochrome *f* in the encounter complex is much more restricted than the negative surface of *P. laminosum* Cyt *f*. Further examination of the structural origin of the different kinetic behavior of cytochrome *f* from *P. laminosum* and higher plants is the subject of a separate publication (*39*).

ACKNOWLEDGMENT

We are grateful to Barry Honig for making the programs DelPhi II and GRASP available, to Wendy Gibson and Jyl Webster for technical assistance, to Matthew Spencer for advice on statistical analysis, and to William Teale and Jürgen Wastl for their assistance with techniques used within this study.

REFERENCES

1. Moser, C. C., and Dutton, P. L. (1996) in *Protein Electron Transfer* (Bendall, D. S., Ed.) pp 1−21, Bios Scientific Publishers, Oxford.
2. Carrell, C. J., Schlarb, B. G., Bendall, D. S., Howe, C. J., Cramer, W. A., and Smith, J. L. (1999) *Biochemistry 38*, 9590−9599.
3. Martinez, S. E., Huang, D., Szczepaniak, A., Cramer, W. A., and Smith, J. L. (1994) *Structure 2*, 95−105.
4. Sainz, G., Carrell, C. J., Ponamarev, M. V., Soriano, G. M., Cramer, W. A., and Smith, J. L. (2000) *Biochemistry 39*, 9164−9173.
5. Gray, J. C. (1992) *Photosynth. Res. 34*, 359−374.
6. Schlarb, B. G., Wagner, M. J., Vijgenboom, E., Ubbink, M., Bendall, D. S., and Howe, C. J. (1999) *Gene 234*, 275−283.
7. Guss, J. M., and Freeman, H. C. (1983) *J. Mol. Biol. 169*, 521−563.
8. Bond, C. S., Bendall, D. S., Freeman, H. C., Guss, J. M., Howe, C. J., Wagner, M. J., and Wilce, M. C. J. (1999) *Acta Crystallogr. D55*, 414−421.
9. Sykes, A. G. (1991) *Struct. Bonding 75*, 175−224.
10. Stewart, A. C., and Kaethner, T. M. (1983) *Photobiochem. Photobiophys. 6*, 67−73.
11. Schlarb-Ridley, B. G., Bendall, D. S., and Howe, C. J. (2002) *Biochemistry 41*, 3279−3285.
12. Ubbink, M., Ejdebäck, M., Karlsson, B. G., and Bendall, D. S. (1998) *Structure 6*, 323−335.
13. Lee, B. H., Hibino, T., Takabe, T., and Weisbeek, P. J. (1995) *J. Biochem. (Tokyo) 117*, 1209−1217.
14. Kannt, A., Young, S., and Bendall, D. S. (1996) *Biochim. Biophys. Acta 1277*, 115−126.
15. Soriano, G. M., Ponamarev, M. V., Piskorowski, R. A., and Cramer, W. A. (1998) *Biochemistry 37*, 15120−15128.
16. Gong, X.-S., Wen, J. Q., Fisher, N. E., Young, S., Howe, C. J., Bendall, D. S., and Gray, J. C. (2000) *Eur. J. Biochem. 267*, 3461−3468.

17. Crowley, P. B., Otting, G., Schlarb-Ridley, B. G., Canters, G. W., and Ubbink, M. (2001) *J. Am. Chem. Soc. 123*, 10444−10453.
18. Wagner, M. J., Packer, J. C. L., Howe, C. J., and Bendall, D. S. (1996) *Biochim. Biophys. Acta 1276*, 246−252.
19. Ausubel, F., Brent, R., Kingston, R. E., Moore, D. D., Seidman, J. G., Smith, J. A., and Struhl, K. (1993) in *Current Protocols in Molecular Biology*, John Wiley, New York.
20. Ponamarev, M. V., Schlarb, B. G., Howe, C. J., Carrell, C. J., Smith, J. L., Bendall, D. S., and Cramer, W. A. (2000) *Biochemistry 39*, 5971−5976.
21. Braman, J., Papworth, C., and Greener, A. (1996) *Methods Mol. Biol. 57*, 31−44.
22. Arslan, E., Schulz, H., Zufferey, R., Kunzler, P., and Thoeny-Meyer, L. (1998) *Biochem. Biophys. Res. Commun. 251*, 744−747.
23. Watkins, J. A., Cusanovich, M. A., Meyer, T. E., and Tollin, G. (1994) *Protein Sci. 3*, 2104−2114.
24. Gilson, M. K., and Honig, B. (1988) *Proteins 4*, 7−18.
25. Sitkoff, D., Sharp, K. A., and Honig, B. (1994) *J. Phys. Chem. 98*, 1978−1988.
26. Wells, J. A. (1991) *Methods Enzymol. 202*, 390−411.
27. Taylor, J. R. (1997) *An Introduction to Error Analysis*, 2nd ed., University Science Books, Sausalito, CA.
28. Schreiber, G., and Fersht, A. R. (1995) *J. Mol. Biol. 248*, 478−486.
29. Northrup, S. H., and Erickson, H. P. (1992) *Proc. Natl. Acad. Sci. U.S.A. 89*, 3338−3342.
30. Janin, J. (1997) *Proteins 28*, 153−161.
31. Vijayakumar, M., Wong, K.-Y., Schreiber, G., Fersht, A. R., Szabo, A., and Zhou, H.-X. (1998) *J. Mol. Biol. 278*, 1015−1024.
32. Gabdoulline, R. R., and Wade, R. C. (1999) *J. Mol. Recognit. 12*, 226−234.
33. Camacho, C. J., Kimura, S. R., Delisi, C., and Vajda, S. (2000) *Biophys. J. 78*, 1094−1105.
34. Selzer, T., and Schreiber, G. (2001) *Proteins 45*, 190−8.
35. Bendall, D. S. (1996) in *Protein Electron Transfer* (Bendall, D. S., Ed.) pp 285−293, Bios Scientific Publishers, Oxford.
36. Kraulis, P. J. (1991) *J. Appl. Crystallogr. 24*, 946−950.
37. Merritt, E. A., and Murphy, M. E. P. (1994) *Methods Enzymol. 277*, 505−524.
38. Nicholls, A., Sharp, K. A., and Honig, B. (1991) *Proteins 11*, 281−296.
39. Schlarb-Ridley, B. G., Bendall, D. S., and Howe, C. J. (2003) *Biochemistry*, in press.

BI020674H